Lasers in Surgery and Medicine 12:471–477 (1992)

Effect of the ArF Excimer Laser on Human Enamel

Osnat Feuerstein, DMD, Daniel Palanker, MSc, Amihay Fuxbrunner, MSc, Aaron Lewis, PhD, and Dan Deutsch, PhD

Dental Research Unit, Hebrew University-Hadassah Faculty of Dental Medicine, Jerusalem 91010 (O.F., D.D.), Hadassah Laser Center, Hadassah-University Hospital, Jerusalem 91120 (A.F.), Division of Applied Physics, Hebrew University, Jerusalem 91904 (D.P., A.L.), Israel

Human enamel surface was irradiated with ArF excimer laser and examined under light microscopy and scanning electron microscopy (SEM). Enamel surface was irradiated at three different areas with different energy fluences. It is demonstrated that the ArF excimer laser causes ablation of the calcified hard enamel tissue. Ablation curves were measured. There was no significant difference found in the etch depth between the three different areas of enamal surface. The morphology of the irradiated areas seen under the SEM was found to be dependent on energy fluence. It changed with increase in energy fluence from being etched to forming a smooth, fused, glaze-like surface and then at very high energy fluences producing a rough surface. The influence of the laser irradiation was confined to the irradiated area only, with no visible heat damage to the surroundings. These results suggest that excimer laser could be applied in a controlled and defined manner for tooth enamel treatments in dentistry.

Key words: laser irradiation, scanning electron microscope, tooth enamel, photoablation, 193 nm excimer laser

INTRODUCTION

Interest in the use of lasers in dentistry has been increasing since 1964 [1,2]. Treatment of tooth enamel with the ruby laser with a wavelength of 694 nm showed a crater-like morphology surrounded by a glass-like appearance at the irradiated zone [1–6], which seems to be caused by fusing, melting, and recrystallization of enamel crystallites. The exposure of human teeth to a ruby laser caused the surface enamel to be more resistant to subsurface demineralization in vitro [7]. Further studies, however, revealed a severe irreversible damage to the pulp as a result of excessive heating [4, 8–10]. The use of other lasers such as the Nd:YAG laser (wavelength of 1,060 nm) and CO_2 laser (wavelength of 10,600 nm) was therefore suggested [11,12].

Structural and phase changes in surface enamel were observed after interaction with CO_2 laser light characterized by a thermal mechanism [13–25]. Similar results were obtained after tooth enamel irradiation with low energy lasers, such as q-switched Nd:YAG [26,27], and argon laser [29]. The effect of these physicochemical changes in tooth enamel confirmed increasing resistance to subsurface demineralization [7, 21–23, 27–31]. There was an attempt to apply the CO_2 laser in a dental clinic replacing the drilling machine for caries removal, sterilization, dentin repair, and increasing resistance to caries [32,33]. However, cracking and carbonization of the irradiated surface with damage of the pulp tissues were observed due to heat conduction during the laser tissue interaction [34–36]. Laser application in

Accepted for publication May 8, 1992.

Address reprint requests to Dan Deutsch, Dental Research Unit, Hebrew University-Hadassah Faculty of Dental Medicine, Israel, Jerusalem 91010, P.O.B. 1172.

dentistry was therefore limited to preventive dentistry.

Recent studies have focused on the Er:YAG, which is a pulsed laser with a wavelength of 2.94 μm. This laser was effectively applied to remove dentin and enamel with minimal damage of the surrounding tissue [37,38]. The rationale for using the Er:YAG is principally concerned with the strong water absorption at this wavelength, which results in a micron-size absorption depth, and partially selective interaction with tissue having high water content.

An alternate strategy for laser applications in dentistry is the use of excimer lasers. The initial study with this laser was concentrated on the use of the XeCl excimer laser at 308 nm for the treatment of dental root canals [39]. All the excimer lasers and especially the argon fluoride excimer laser at 193 nm are characterized by its nonthermal photoablation interaction with polymers [40,41], and, therefore, it seemed to be an effective solution for laser irradiation of tooth enamel without thermal damage to the pulp. At such a wavelength, the covalent chemical bonds absorb radiation and enter an excited state in which there is a dissociation without significant deposition of heat.

In this preliminary study, we examined the etch depth and surface morphology of mature, human enamel treated by 193 nm excimer laser at seven different energy fluences ranging from 250 to 650 mJ/cm^2. The results established a correlation between etch depth per pulse, different morphology of irradiated surface, and energy fluence.

MATERIALS AND METHODS

Preparation of Tooth Enamel for Laser Irradiation

A total of 42 longitudinal sections of ~ 0.7 mm in thickness were prepared from four sound human wisdom teeth (III molars), from the tip of the crown to the cervical margin, with a Beuhler diamond low speed sectioning machine. Immediately after extraction the teeth were carefully cleaned from soft tissue and blood under dissecting microscope using soft tissue paper to avoid any damage to the enamel surface. The tooth regions selected for laser irradiation were covered with sound enamel with no obvious caries or any other malformations.

Approximately 10 parallel longitudinal (from mesial to distal) sections were made from each tooth, and the enamel surface was irradiated and analyzed as described below.

Irradiation of Enamel Surface With Excimer Laser

A Lamda Physik Model EMG 103 MSC ArF excimer laser was used with a wavelength of 193 nm and a pulse duration of 20 ns. The irradiation spot size was fixed to 1 mm in diameter by a metal mask. The laser beam was concentrated with a convex cylindrical lens and passed through this mask at average powers of −25,30,35,40,45, and 50 mw with energy fluences ranging from 300 to 650 mJ/cm^2 per pulse respectively. Laser beam power was measured with the DGX Laser Power/Energy Meter, Ophir Ltd (Jerusalem, Israel). Seven sections were irradiated at each energy fluence. Each longitudinal section was irradiated in three regions: occlusal enamel, medial enamel, and cervical enamel, i.e., a total of 126 enamel regions were irradiated. The sections were fixed to a special holder that could be moved on an optic bench relative to the metal mask. They were irradiated at 10Hz for 4,000 pulses.

Etch Depth Measurement

A total of 252 etch depth measurements were made from 126 profiles of irradiated areas (two for each irradiated enamel region) using a scaled binocular microscope (accuracy of ± 3 μm).

Examination of Irradiated Enamel With Scanning Electron Microscope (SEM)

Human enamel specimens irradiated with the excimer laser at seven different energy fluences and an untreated specimen used as control were examined under JEOL 840 Scanning Electron Microscope at 15KV.

The samples were attached, with epoxy resin, to aluminium stubs then sputtered with ~ 200Å thick layer of carbon.

RESULTS

Etch Depth Measurement

The etch depth of each irradiated enamel area can be seen in Table 1. These data were analyzed using an analysis of covariance model. The results show that as the energy fluence increased so did the etch depth of the irradiated enamel ($p = 0.0001$) measured at three different regions: occlusal, medial and cervical (Fig. 1). No significant difference was observed in the etch depth between the three regions at the same energy fluences ($p = 0.1457$).

TABLE 1. Etch Depths of Each Irradiated Enamel Area at Different Energy Fluences

Energy fluence mJ/cm^2 (± $25mJ/cm^2$)	Etch depth of occlusal area (nm/pulse)	Etch depth of medial area (nm/pulse)	Etch depth of cervical area (nm/pulse)	Etch depth of average of the areas (nm/pulse)
318	2.5 ± 1.0	2.3 ± 0.8	2.5 ± 1.8	2.5 ± 1.3
382	4.5 ± 1.5	3.5 ± 1.3	4.3 ± 1.0	4.0 ± 1.3
446	11.5 ± 3.5	10.8 ± 5.8	12.8 ± 5.5	11.5 ± 5.0
510	17.5 ± 3.3	16.3 ± 6.0	15.8 ± 5.3	16.5 ± 5.0
573	22.2 ± 8.0	19.3 ± 4.0	19.8 ± 5.5	20.3 ± 6.0
637	28.8 ± 6.0	26.3 ± 7.0	26.5 ± 4.3	27.3 ± 5.8

Scanning Electron Microscopy (SEM)

The surface morphology of occlusal enamel produced by a 10Hz, 4,000 pulses laser treatment of intact human enamel at seven different energy fluences can be seen in Figure 1. The enamel was examined at the center as well as at the periphery of the irradiated areas.

The control enamel surface, without laser irradiation, shown at low magnification (Fig. 1 control(i)), is a relatively structureless layer of enamel with transverse wavelike grooves, perikymata, believed to be the external manifestations of the striae of Retzuis. At higher magnification (Fig. 1 control(ii)) rod ends, cracks, and micropores were observed.

The low 255 ± 25 mJ/cm^2 energy fluence laser treatment of enamel (Fig. 1a) produced very slight erosion observed under low magnification exhibited a delicate periodic surface roughening with a bright halo of ~ 100 μm width around the irradiated area. At this magnification, the perikymata were still visible transversing both the irradiated and unirradiated areas (Fig. 1a(i)). At higher magnification (Fig. 1a(ii)) the outer prism free layer and the rod boundaries were removed, resembling an etching pattern resulting from an acid treatment of enamel surface where the rod peripheries are preferentially eroded leaving the rod core intact. At the periphery of the irradiated area, 3–5 concentric lines of rod ends were observed (Fig. 1a(i)). A narrow layer of micro particles, probably from the ablated material, was covering the enamel surface around the boundaries of the irradiated area (Fig. 1a(i)).

The 318 ± 25 mJ/cm^2 energy fluence treatment (Fig. 1b) (etch depth of 10 ± 5 μm) produced a surface etching morphology resembling that of the 255 mJ/cm^2 energy fluence. At low magnification, the periodic surface roughening of the irradiated area and the bright halo around it were observed (Fig. 1b(i)). At higher magnification (Fig. 1b(ii)) the rod boundaries were partially removed and it appeared that adjacent rod ends were joined together. The layer of ejected material around the irradiated area appeared to be melted and cracked (Fig. 1b(i)).

The 382 ± 25 mJ/cm^2 energy fluence treatment (Fig. 1c) (etch depth of 16 ± 5 μm) produced a rough area, less periodic when compared to either of the 255 mJ/cm^2 and 318 mJ/cm^2 energy fluence treatments. At low magnification the roughed irradiated area and the bright halo around it were observed (Fig. 1c(i)). At high magnification (Fig. 1c(ii)) the irradiated area gave the appearance of partially fused rod ends with a network of crystallites above and between the rod ends. A covering cracked fused layer around the irradiated area might be ablated material that was melted and got quickly solidified on the surrounding surface (Fig. 1c(i)).

The 446 ± 25 mJ/cm^2 energy fluence treatment (Fig. 1d) (etch depth of 46 ± 20 μm) produced a periodic arranged area that at low magnification (Fig. 1d(i)) exhibited a pattern of rounded clusters, each ~ 70 μm in diameter. At higher magnification (Fig. 1d(ii)) the rounded clusters were made of fused melted rod ends with some areas that were covered also by a network of crystallites. The melted surface exhibited very little micropores, ~ 100–200 nm in diameter. The surface around the irradiated area, for a distance of more than 200 μm, was partially covered by what appeared to be the ablated material (Fig. 1d(i)).

The 510 ± 25 mJ/cm^2 energy fluence treatment (Fig. 1e) (etch depth of 66 ± 20 μm) produced a coarse roughening that at low magnification (Fig. 1e(i)) exhibited no special pattern in comparison to 446 mJ/cm^2 energy fluence treatment. At higher magnification (Fig. 1e(ii)) the irradiated area, although rough, was partially covered also by a smooth fused glazelike surface. The

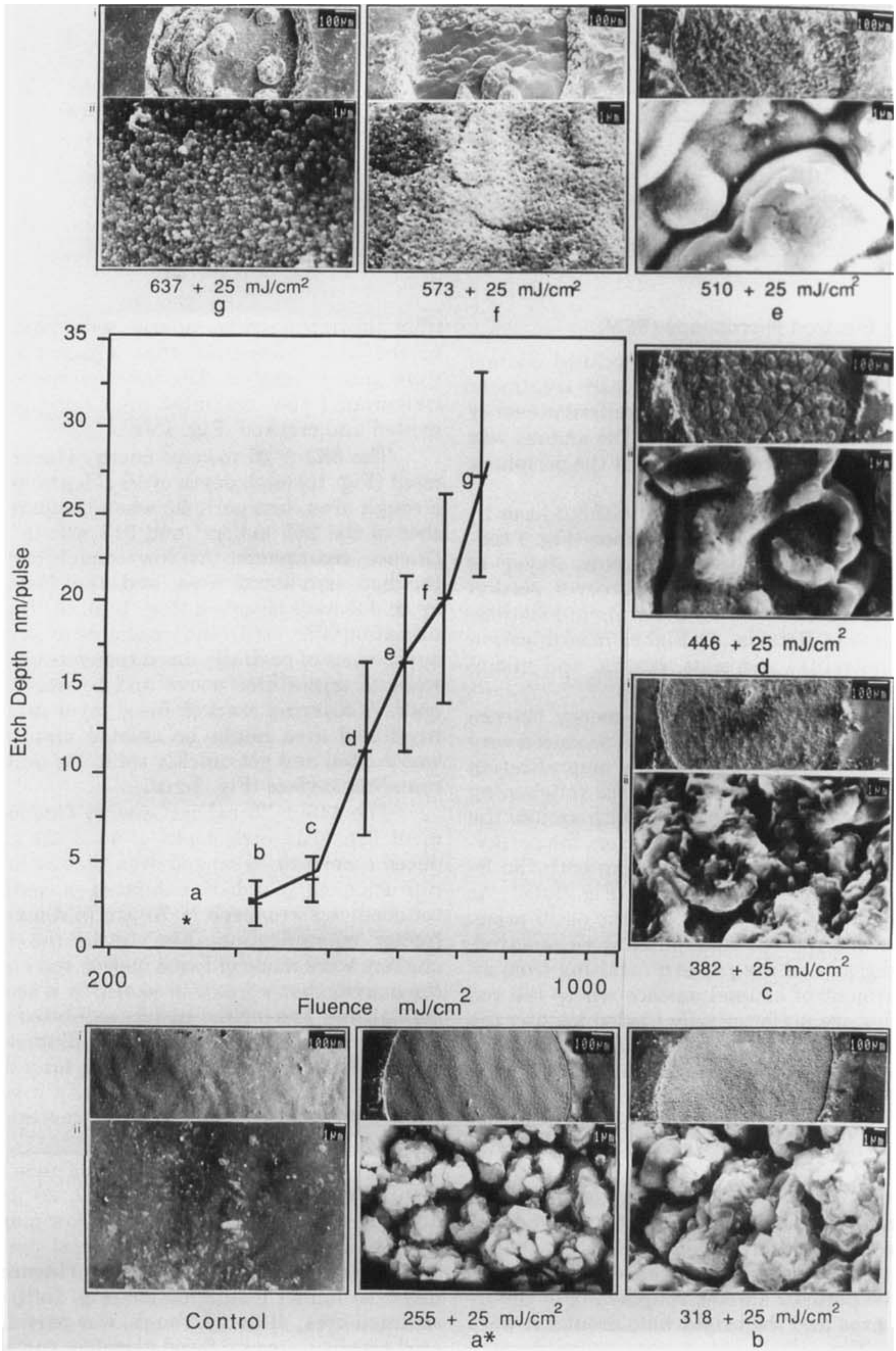
637 + 25 mJ/cm²
g
573 + 25 mJ/cm²
f
510 + 25 mJ/cm²
e
446 + 25 mJ/cm²
d
382 + 25 mJ/cm²
c
Control
255 + 25 mJ/cm²
a*
318 + 25 mJ/cm²
b
Etch Depth nm/pulse
Fluence mJ/cm²
200
1000
0
5
10
15
20
25
30
35

Fig. 1.

melted surface exhibited also the same micropores as described with the 446 mJ/cm^2 energy fluence treatment. Some particles from the ablated material covered the surface around the irradiated zone (Fig. 1e(i)).

The 573 ± 25 mJ/cm^2 energy fluence treatment (Fig. 1f) (etch depth of 81 ± 24 μm) produced a smooth area that at low magnification (Fig. 1f(i)) exhibited a smooth fused glazelike surface. At higher magnification (Fig. 1f(ii)) a delicate pattern of the rod ends that had the appearance of horseshoes were observed (also described in decalcified enamel section). The micropores of the melted surface were even more prominent than with the 446 or 510 mJ/cm^2 energy fluence treatment. The surface around the irradiated area, for a distance of more than 200 μm, was covered with a fused layer that appeared to be the ablated material, which was melted and solidified on that surface (Fig. 1f(i)).

The 637 ± 25 mJ/cm^2 energy fluence treatment (Fig. 1g) (etch depth of 109 ± 23 μm) produced rough area that at low magnification appeared partially smooth (Fig. 1g(i)). At higher magnification (Fig. 1g(ii)) small projections, ~ 300 nm in diameter covered the surface. Around the irradiated area some particles from the ablated material were observed on the surface (Fig. 1g(i)).

DISCUSSION

The present results, which are concerned with effects of the ArF excimer laser on the surface of mature erupted enamel, indicate that short pulses (20 nsec) of 193 nm laser radiation produce a defined ablation not only of the organic but also of the mineral component of the hard enamel tissue.

The mature enamel consists mainly of inorganic material [96% (w/w)] and only a small amount of organic substance and water [4% (w/w)]. The enamel is composed of apatite crystals arranged in enamel rods or prisms with a very small amount of organic material surrounding them. The interprismatic material is termed the rod sheaths.

Two distinguished morphologies of the irradiated enamel areas were observed under the SEM; an etching produced by low energy fluences of the irradiation (255–382 ± 25 mJ/cm^2) (Fig. 1a–c), which was probably mainly due to a nonthermal ablation process of the organic rod sheaths and mineral, and a second type of morphology produced by higher energy fluences of irradiation (446–637 ± 25 mJ/cm^2) (Fig. 1d–g), which exhibited features of melting. The surfaces become smoother with increasing energy fluence from 446 ± 25 mJ/cm^2 (Fig. 1d) to 573 ± 25 mJ/cm^2 (Fig. 1f). At higher energy fluence (637 ± 25 mJ/cm^2) (Fig. 1g) a different morphology is observed.

From an energy fluence of 446 ± 25 mJ/cm^2 to 573 ± 25 mJ/cm^2, it appears as if the process includes an increasing proportion of heating that results in melting of a thin surface layer. The transition from 510 ± 25 mJ/cm^2 to 573 ± 25 mJ/cm^2 results in a pronounced change in the surface appearance after laser irradiation: a series of fairly uniform holes can be seen to emerge over the whole irradiated area. At this energy the melted layer becomes thicker and can fill the interprismatic spaces resulting in a fairly uniform surface. Within this uniform surface appears a network of micropores with a typical diameter of 100–200 nm and with a distance between them of submicron dimension. This structure is less obvious at lower energies and only becomes fully apparent at energy level around 573 ± 25 mJ/cm^2. At even higher energies this surface becomes less regular, and this probably results from partially melted fragments that fall down on the surface from the cloud of ejected material and stick to the irradiated region. If such an explanation is correct, it is expected that at even higher energies a smooth surface will once again form due to the presence of a larger degree of melted material and the longer time that is required for cooling.

The present results of higher energy fluence irradiation with the ArF excimer laser resemble in appearance the thin smooth fused surface layer and the underlying rougher enamel observed with the IR lasers [6,11,21,22,28]. Tagomori and Morioka [28] suggested a rapid melting and subsequent resolidification of the enamel crystals,

Fig. 1. Etch depth per pulse plotted against energy fluence logarithm for the average of occlusal, medial, and cervical areas of human sound enamel(**). Scanning electron micrographs [a–g(i–ii)] of the irradiated occlusal enamel surfaces are related to the plotted points by letters. (i) = magnification ×20; (ii) = magnification ×1,000. *No measurements of etch depth were taken for energy fluence of 255 ± 25 mJ/cm^2, because the resolution of the method was not enough for that slight etch depth.

when a long pulse (0.3 msec) Nd:YAG laser was used. Nelson et al. [22], who used a pulsed CO_2 laser with a pulsed width similar to Tagomori and Morioka [0.1–0.2 msec), suggested that the surface roughening may be caused by preferential surface melting or by the rapid thermal cycles during laser irradiation. Despite the resemblance of our ArF excimer laser results to these earlier IR laser investigations, there were also some substantial differences. The interaction of UV laser pulses (ArF excimer) with enamel was distinguished from that of IR laser by the sharply defined boundaries with a geometry that is defined by the light beam without charring or detectable damage to the surrounding. Enamel irradiated with the ArF excimer laser did not contain surface features such as cracks, surface flaking, and craters typical of IR lasers irradiated enamel, which were explained by stresses in enamel due to expansion and contraction through localized heating and shock waves associated with the beam's interaction with the tooth [25].

Another typical feature of UV laser is the control over the depth of the etching by defining the number of pulses and the energy fluence of the laser. The typical shape of the etch depth plot (see Fig. 1) indicates that at low energy fluences the initial curve region approaches the abscissa asymptotically. This is followed by a region of energy fluences in the range of $446–637 \pm 25$ mJ/cm^2, where the etch depth per pulse is linear with energy fluence logarithm. In this linear region of energy fluences the morphology of the irradiated enamel exhibits the features of melting.

From the results obtained, it seems reasonable that by controlling the energy fluence of the laser beam, it would be possible to sterilize and selectively remove carious enamel without considerable damage to the surrounding sound enamel. The laser technique might be useful for treatment of carious and noncarious (preventive treatment) of pits and fissures that are hard to reach with the conventional technique.

Low energy fluence irradiation, which results in etching of the enamel surface, could provide mechanical retention for dental restorative materials with a defined area and depth. Frentzen and Koort [42], e.g., have demonstrated that the bond strength values of composites with ArF excimer laser irradiated surfaces corresponded to ~ 75% of those obtained by acid etching techniques.

Higher energy fluences laser irradiation of enamel produces a smooth melted surface. Studies with IR laser irradiation had shown that similar smooth melted surfaces were more resistant to subsurface demineralization [7,21–23,27–31]. These studies also showed [28] that treatment of enamel surface with fluoride solution after laser irradiation increased uptake of fluoride into surface enamel.

Work is proceeding in an attempt to establish the precise morphological and chemical changes that occur on sound enamel in order to understand the ablation mechanism that is believed to be a mixture of photochemical and photothermal dissociation and to verify the potential of this laser in dentistry.

ACKNOWLEDGMENTS

We thank Mr. Michael Dvorachek from the Geological Survey of Israel for his assistance with the SEM work, and Mrs. Laura J. Rosen from the Hebrew University for her assistance with the statistical analysis of the results.

REFERENCES

1. Goldman L, Hornby P, Meyer R, Goldman B. Impact of the laser on dental caries. Nature 1964; 4943:417.
2. Stern RH, Sognnaes RF. Laser beam effect on dental hard tissues. J Dent Res 1964; 43(Suppl. to No. 5):873, Abstract 307.
3. Sognnaes RF, Stern RH. Laser effect on resistance of human dental enamel to demineralization in vitro. J S Calif Dent Assoc 1965; 33:328–329.
4. Taylor R, Shklar G, Roeber F. The effects of laser radiation on teeth, dental pulp and oral mucosa of experimental animals. Oral Surg 1965; 19:786–795.
5. Lobene RR, Fine S. Interaction of laser radiation with oral hard tissues. J Prosthet Dent 1966; 16:589–597.
6. Vahl J, Pfefferkorn G. Electron optic studies of changes in the dental hard substance caused by laser irradiation. Dtsch Zahnaerztl Z 1967; 22:386–394.
7. Stern RH, Sognnaes RF, Goodman F. Laser effect on in vitro enamel permeability and solubility. J Am Dent Assoc 1966; 73:838–843.
8. Stern RH, Renger HL, Howell FV. Laser effects on vital dental pulps. Br Dent J 1969; 127:26–28.
9. Adrian JC, Bernier JL, Sprague WG. Laser and the dental pulp. J Am Dent Assoc 1971; 83:113–117.
10. Yamamoto H, Okabe H, Ooya K, Hanaoka S, Ohta S, Kataoka K. Laser effect on vital oral tissues: A preliminary investigation. J Oral Pathol 1972; 1:256–264.
11. Stern RH, Vahl J, Sognnaes RF. Lased enamel: ultrastructural observations of pulsed carbon dioxide laser effects. J Dent Res 1972; 51:455–460.
12. Adrian JC. Pulp effect of neodymium laser. A preliminary report. Oral Surg 1977; 44:301–305.
13. Lobene RR, Bhussry BR, Fine S. Interaction of carbon dioxide laser radiation with enamel and dentin. J Dent Res 1968; 47:311–317.

14. Vahl J. Electron microscopical and X-ray crystallographic investigations of teeth exposed to laser rays. Caries Res 1968; 2:10–18.
15. Kantola S. Laser induced effects on tooth structure. Electron probe microanalysis and polarized light microscopy of dental enamel. Acta Odontol Scand 1972b; 30:475–484.
16. Kantola S, Laine E, Tarna T. Laser induced effects on tooth structure. VI. X-ray diffraction study of dental enamel exposed to a CO_2 laser. Acta Odontol Scand 1973; 31:369–379.
17. Kuroda S, Nakahara H. Morphological changes in laser-irradiated extracted teeth. J Dent Res 1981; 60 (special issue A): Abstract 719.
18. Kuroda S, Fowler BO. Compositional, structural and phase changes in in vitro laser-irradiated human tooth enamel. Calcif Tissue Int 1984; 36:361–369.
19. Newesely H. High temperature behaviour of hydroxy and fluorapetite. Crystalchemical implications of laser effects on dental enamel. J Oral Rehabil 1977; 4:97–104.
20. Fowler BO, Kuroda S. Changes in heated and in laser-irradiated human tooth enamel and their probable effect on solubility. Calcif Tissue Int 1986; 38:197–208.
21. Nelson DGA, Jongebloed WL, Featherstone JDB. Laser irradiation of human dental enamel and dentin. N Z Dent J 1986a; 82:74–77.
22. Nelson DGA, Wefel JS, Jongebloed WL, Featherstone JDB. Morphology, histology and crystallography of human dental enamel treated with pulsed low-energy infrared laser irradiation. Caries Res 1987; 21:411–426.
23. Featherstone JDB, Nelson DGA. Laser effects on dental hard tissues. Adv Dent Res 1987; 1:21–26.
24. Sakae T. X-ray diffraction and thermal studies of crystals from the outer and inner layers of human dental enamel. Archs Oral Biol 1988; 33:707–713.
25. Ferreira JM, Palamara J, Phakey PP, Rachinger WA, Orams HJ. Effects of continuous-wave CO_2 laser on the ultrastructure of human dental enamel. Archs Oral Biol 1989; 34:551–562.
26. Yamamoto H, Ooya K. Potential of Yttrium-aluminium-garnet laser in caries prevention. J Oral Pathol 1974; 3:7–15.
27. Yamamoto H, Sato K. Prevention of dental caries by Nd: YAG laser irradiation. J Dent Res 1980; 59:2171–2177.
28. Tagomori S, Morioka T. Combined effects of laser and fluoride on acid resistance of human dental enamel. Caries Res 1989; 23:225–231.
29. Goodman BD, Kaufman HW. Effects of an argon laser on the crystalline properties and rate of dissolution in acid of tooth enamel in the presence of sodium fluoride. J Dent Res 1977; 56:1201–1207.
30. Stern RH, Sognnaes RF. Laser inhibition of dental caries suggested by first tests in vivo. J Am Dent Assoc 1972; 85:1087–1090.
31. Nelson DGA, Shariati M, Glena R, Shields CP, Featherstone JDB. Effect of pulsed low energy infrared laser irradiation on artificial caries-like lesion formation. Caries Res 1986b; 20:289–299.
32. Melcer J, Chaumette MT, Melcer F, Dejardin J, Hasson R, Merard R, Pinaudeau Y, Weill R. Treatment of dental decay by CO_2 laser beam: Preliminary results. Laser in Surgery and Medicine 1984; 4:311–321.
33. Melcer J. Latest treatment in dentistry by means of the CO_2 laser beam. Laser in Surgery and Medicine 1986; 6:396–398.
34. Boehm R, Rich J, Webster J, Janke S. Thermal stress effects and surface cracking associated with laser use on human teeth. J Biomech Eng 1977; 99:189–194.
35. de Raad M, Paschoud Y, Holz J. Effects du Laser a CO_2 sur les tissues Dentaires. J Biol Buccale 1988; 16:137–150.
36. Jeffrey IWM, Lawrenson B, Saunders EM, Longbottom C. Dentinal temperature transients caused by exposure to CO_2 laser irradiation and possible pulpal damage. J Dent 1990; 18:31–36.
37. Hibst R, Keller U. Experimental studies of the application of the Er:YAG laser on dental hard substances: I. Measurement of the ablation rate. Lasers Surg Med 1989; 9:338–344.
38. Keller U, Hibst R. Experimental studies of the application of the Er:YAG laser on dental hard substances: II. Light microscopy and SEM investigation. Lasers Surg Med 1989; 9:345–351.
39. Pini R, Salimbeni R, Vannini M, Barone R, Clauser C. Laser dentistry: A new application of excimer laser in root canal therapy. Lasers Surg Med 1989; 9:358–361.
40. Srinivasan R, Mayne-Banton V. Self-developing photoetching of poly(ethylene terephthalate) films by far ultraviolet excimer laser radiation. Appl Phys Lett 1982; 41:576.
41. Srinivasan R, Leigh WJ. Ablative photodecomposition: Action of far-ultraviolet(193nm) laser radiation on poly(ethylene terephthalate) films. J Am Chem Soc 1982; 104:6784.
42. Frentzen M, Koort HJ. Preparation of hard tooth structure with excimer lasers. Dtsch Zahnarztl Z 1989; 44(6): 454–457.